Giant Gold−Glutathione Cluster Compounds: Intense Optical Activity in Metal-Based Transitions

T. Gregory Schaaff*,† and Robert L. Whetten‡

School of Chemistry and Biochemistry and School of Physics, Georgia Institute of Technology, Atlanta, Georgia 30332-0430

Received: October 18, 1999; In Final Form: January 10, 2000

A series of giant metal-cluster compounds, each composed of a gold core and a glutathione (GSH) adsorbate layer, have been prepared from Au(I)SG polymers and separated by gel electrophoresis, using methods reported in a recent Letter [*J. Phys. Chem. B* **1998**, *102*, 10643−6]. Identification of the separated compounds by core mass is accomplished through laser desorption mass spectrometry of matrix-diluted films. Three principal compounds have core masses of ca. 4.3, 5.6, and 8.2 kDa (in the range of ∼20−40 Au atoms), and show structured optical absorption spectra with clear optical absorption onsets near 1.7, 1.3, and 1.0 eV, respectively. Each of these shows unusually strong chiroptical activity in the metal-based electronic transitions across the near-infrared, visible, and near-ultraviolet regions, whereas neither the crude (unseparated) mixture nor its higher molecular weight components possess such strong optical activity. The location and strength of the optical activity suggest a metal electronic structure that is highly sensitive to the chiral environment imposed by the glutathione adsorbate groups, if indeed the gold core is not inherently chiral. Mechanisms that could account for the observed optical activity are discussed, but the mere presence of strong chiroptical effects in this metallic-cluster system places these novel compounds in a special class of molecular substances. Previously known giant metal-cluster compounds (and nanocrystals) have not been reported to exhibit significant optical activity. With these results, there emerges a rather complete picture of the evolution of optical and electronic properties of thiol-based gold cluster compounds (or self-assembled monolayer passivated gold nanocrystals) from 20 to 1000 Au atoms (0.7−3.2 nm core diameter).

Introduction

The striking electronic and optical properties of nanometer-scale metal crystallites—as colloids or giant clusters and cluster compounds—arise mainly from the electrons in orbitals of the partially filled conduction band, i.e., from electronic states that are delocalized throughout the metal nanostructure.[1] When the diameter of such nanocrystals is reduced to the order of the metal's Fermi wavelength (∼0.5 nm for Au), then quantization of these orbital energy levels is important even under ambient conditions, with profound consequences for optical, electronic, charging, and transport phenomena, such as the "Coulomb staircase" response in single electronics.[2] At the same time, catalytic and electrocatalytic activity is enhanced, in the long-known catalytic metals such as platinum,[3] or can emerge dramatically, in the case of gold.[4] Enhanced optical properties include intense color or iridescence in transmission and reflection, and strong nonlinear or electrooptical effects;[5] these form the basis for applications including colorimetric probes and sensors.[6] Finally, at sufficiently small metallic cluster sizes, the continuous optical spectra, including the broad "collective resonances" (plasmons), give way to discrete electronic transitions among quantized levels, each associated with a delocalized orbital.[1,7]

The actual form of the conduction-band orbitals, and hence the optical and electronic properties derived therefrom, are dictated by the symmetry of the lattice structure of the metal, as well as its shape (morphology) and the surface structure and bonding. Usually, one has found or assumed these structures to be either fragments of the bulk crystal lattice or symmetrically adjoined or twinned combinations of such fragments (e.g., fcc-derived truncated octahedra[8] or truncated pentagonal-decahedra[9]). Such considerations would rule out the possibility of topologically interesting structures, such as those possessing a helical or chiral character. However, calculations performed by Wetzel and DePristo,[10] which have found experimental support,[11] indicate that the 39-atom Ni cluster prefers a lower (D_5) symmetry that would give rise to optical activity. Similarly, metal nanowires of sufficiently small diameter (less than six atoms in diameter) have been predicted to preferentially assume helical structures with close-packed surface layers.[12] Analogous low-symmetry (or "reduced-symmetry") structures are already established for the case of semimetallic (graphitic) carbon, i.e., larger chiral fullerenes[13] and carbon nanotubes.[14]

In the case of small Au nanocrystals and their large and giant cluster compounds, comprising some 20−200 or so atoms, the structural evidence has been interpreted as being consistent with structures of the simpler variety, in particular the cylindrical-type (D_{5h}) truncated decahedra,[9b] with compact metal cores slightly dilated by interactions with the weakly binding adsorbate groups. The optical spectra of these recently isolated Au:SR and Au:PR_3 compounds are richly structured in both the low-energy "intraband" region (<1.8 eV, >700 nm, corresponding to transitions within the partially filled Au 6sp conduction band), as well as in the "interband" region (>1.8 eV), which is dominated by transitions from the buried Au 5d orbitals to the

† School of Chemistry and Biochemistry. Present address: Chemical and Analytical Sciences Division, Oak Ridge National Laboratory, Oak Ridge, TN 37831-6365. Phone: (865) 574−4857. Fax: (865) 576-8559. E-mail: schaaffg@ornl.gov.

‡ School of Chemistry and Biochemistry and School of Physics. E-mail: Whetten@chemistry.gatech.edu.

10.1021/jp993691y CCC: $19.00
Published on Web 02/24/2000

SCHEME 1

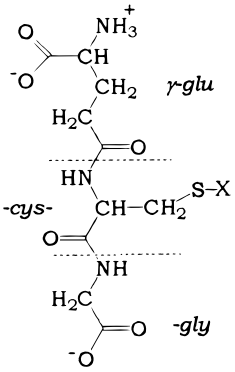

unoccupied conduction band orbitals.[7,15] These new compounds present a timely opportunity for detailed exploration of electronic and spectroscopic phenomena in very small metallic particles.

In a recent brief Letter,[16] we reported that very small gold nanocrystals (giant clusters) can be obtained in robust hydrophilic forms when the adsorbate monolayer is assembled from the sterically demanding GS group, where GSH denotes the ubiquitous tripeptide glutathione (γ-glu-cys-gly, Scheme 1). In these Au:SG compounds, the gold core is restricted to $\leq$1.5 nm diameter, but appears to retain the metallic Au^0 character, as evidenced by the Au−Au bond length (0.29 nm), and the tripeptide is adsorbed intact and exclusively via the cysteine sulfur functionality. Electrophoretic separations revealed a particularly abundant component, whose total molecular weight of 10.42 kDa total is consistent with the composition $Au_{28}(SG)_{16}$. This compound forms a molecular crystalline solid, in which the 0.9 nm cores are arranged as a bcc lattice with a 2.0 nm nearest-neighbor distance. Separately, Templeton et al.[17] have developed methods for the hydrophilic Au:tiopronin system and have reported many properties of the mixtures of these cluster compounds. The recently developed preparation and isolation of the hydrophilic Au:SR cluster compounds can be envisioned as an extension of the previously separated Au:SR (R = *n*-alkane) cluster compounds and SAM-passivated gold (and silver) nanocrystal homologues,[7,18] and many of their interesting properties can be directly compared.

The polyelectrolyte character of the Au:SG cluster compounds facilitates the use of characterization methods adopted from molecular biology, including gel electrophoresis separations, and matrix-assisted laser desorption and electrospray ionization mass spectrometry. Through employing these methods, one obtains robust compounds, the smallest of which show striking quantum-size effects, i.e., evidence for electronic level quantization and the emergence of a HOMO−LUMO gap in the near-infrared−visible spectral regions. Furthermore, because the GS adsorbates are obtained from the natural product (L,L configuration), one can obtain additional information regarding the optical electronic bands observed, by means of circular dichroism. Specifically, the large and giant gold cluster compounds prepared with the natural thiol adsorbate glutathione have surprisingly large absolute and relative ($\Delta\epsilon/\epsilon$) optical activity.

Results

The giant gold:glutathione (Au:SG) cluster compounds have been prepared, isolated, characterized, and further investigated by methods described fully in the Appendix (Methods Section). In contrast to the results on the electrophoretically separated compounds shown below, preliminary measurements carried out on mixtures (crude or partially separated) invariably gave quite inferior results. Specifically, the optical absorption spectra of crude mixtures were rather featureless, and the strong chiroptical effects seen for the separated compounds are diminished in the CD spectra of the mixture, as opposite signed CD amplitudes tend to cancel. Thus, only through rigorous separations could the quantum-size effects (electronic level quantization, size-dependent emergence of HOMO−LUMO gap, and optical activity in Au transitions) for these compounds be realized. Therefore, the nomenclature adopted for the purpose of this report is a numbering system based on the electrophoretic mobility of the cluster compounds, i.e., the separated compounds are simply referred to as compounds **1**−**5**, with **1** being the most mobile compound. Naturally, it may also turn out that further separation efforts could resolve additional, minor components, in which case the interesting features revealed herein would be even further enhanced. For example, the CD may be further enhanced by the resolution of a partially racemic mixture.

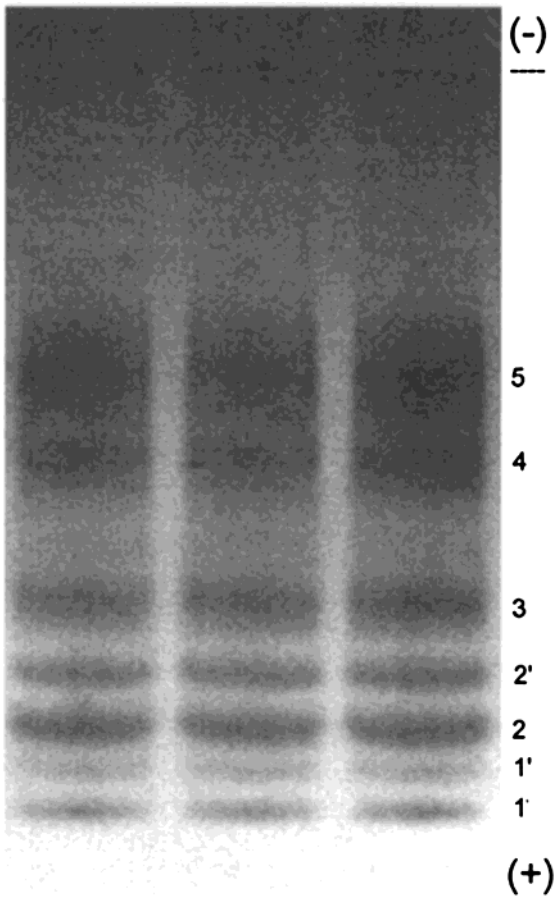

Figure 1. Photograph of PAGE separation. Seven bands were separated by the high density (HD) gel and are labeled in order of mobility (**1** being most mobile). Starting point is indicated by the dashed line at top.

A. Identification of Au:SG Giant Cluster Compounds. *1. Electrophoretic Mobilities*. A photograph of a typical high-density (HD) gel separation is shown in Figure 1. Seven dark bands, or components of the mixture, are readily visible under normal illumination. Under these conditions, the first five bands are sharply defined and the last two are rather diffuse. The use of the low-density (LD) gel reverses the situation (Figure S1, Supporting Information). Repeated electrophoretic separation of individual components confirmed the distinct mobility of each of the seven components, which are quantified in Table 1, and has also been used occasionally to reduce the "tailing" from the intense third band into the less-intense fourth and fifth bands.

TABLE 1: Characteristics of Au:SG Cluster Compounds

band	mobility[a]	% yield	core mass[b] (kDa)	optical gap[c] (eV)
1	1.00	1.7	4	1.7
1′	0.93	6.0		1.7
2	0.87	32.5	6	1.3
2′	0.80	7.3	~7	1.3
3	0.71	7.7	8	1.0
4	0.53	3.5	9[d]	<0.8
5	0.42	9.8	14[d]	<0.8

[a] Relative to band 1. [b] As determined by MALDI-MS. [c] Determined from onset of optical absorption (see Figure 2). [d] Determined from MS of LD gel separation.

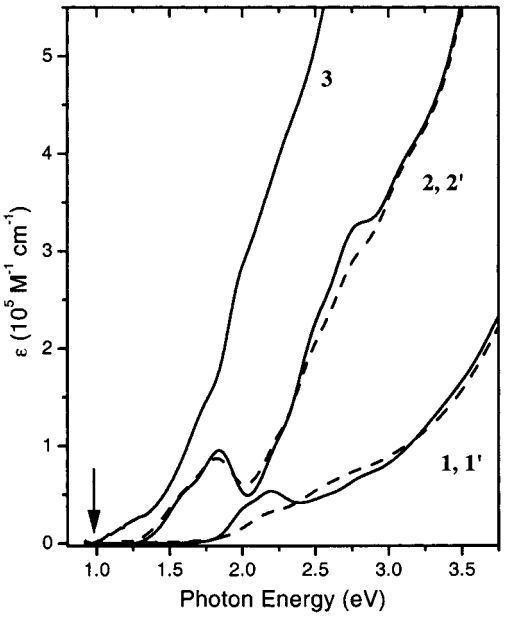

Figure 2. Optical properties of separated Au:SG cluster compounds in the NIR-visible region. Unprimed (primed) numerals refer to solid (dashed) lines.

Table 1 also gives the percent yield of these components, determined gravimetrically, from a preparation optimized for bands of intermediate mobility. Once isolated and purified from the electrophoresis buffers, the resulting cluster compounds are stable, exhibiting unchanging optical spectra and mass spectra, when stored as powders for periods of many months under normal ambience.

2. Spectroscopic Identification. Spectroscopic Differentiation of Au:SG Compounds. The near-IR/visible optical absorption spectra for the first five bands are displayed in Figure 2. The spectra are highly structured, showing clear absorption onset energies at 1.7 eV (two highest-mobility components), 1.3 eV (next two), and 1.0 eV, as summarized in Table 1. (The final two components do not show absorption onsets at energies above 0.8 eV.) The inherent colors observed in the electrophoresis separation of the cluster compounds can be deduced from various minima and maxima in the visible region of the absorption spectra of the cluster compounds. Thus, the optical properties indicate that the compounds are separated by differing core size (with the smallest having the highest mobility), which is consistent with the mass spectrometry, to follow.

The similarities between the spectra of the two highest-mobility components seem too strong to be coincidental, and the same is true of the spectra of the next two components. The most likely explanation is that the lower-mobility component differs from the higher-mobility component only by the loss of a single (or a few) adsorbate group(s), because the electronic structure and optical spectra are determined mainly by the structure of the gold core, whereas the mobility is very sensitive to the number of charged surface groups (carboxylates). For this reason, it seems best to refer to the seven components as compounds **1, 1′**, **2**, **2′**, **3**, **4**, **5**, where the primes refer to the lower-mobility, surface-unsaturated variants of their unprimed counterparts. In the following, though, most attention is devoted to the higher-mobility compounds **1**, **2**, and **3**.

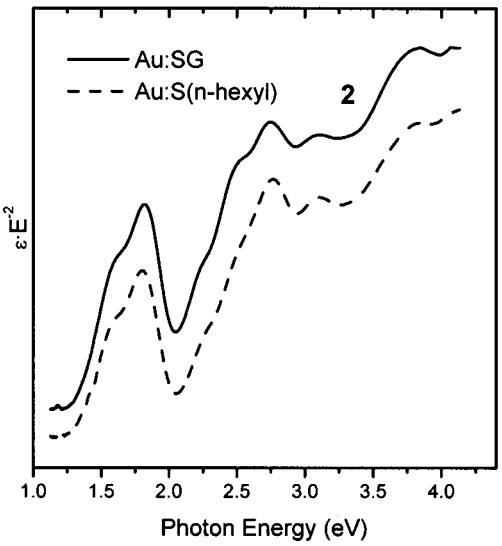

Figure 3. Comparison of optical spectra derived from clusters (with the same approximate core mass of ~5.6 kDa) prepared using glutathione (solid line) and *n*-hexanethiol (dashed line). The spectra have been multiplied by wavelength squared and offset to facilitate comparison in this spectral region.

Spectroscopic Matching to Hydrophobic Au:SR Compounds. The Au-core sizes of the Au:SG cluster compounds extend the core-size range of the Au:SR compounds to smaller sizes than previously achieved (using R = hydrophobic *n*-alkanes).[7a,16] Figure 3 shows a comparison of the spectra from compound **2** and from a Au:S(*n*-hexyl) cluster compound that has approximately the same core mass, as measured by laser desorption mass spectrometry (see Supporting Information and Figure S2). This low yield compound (<1% of total cluster yield) was highly unstable relative to larger Au:S(*n*-hexyl) compounds, degrading under nitrogen within a day. The absorption spectra for the two species are essentially identical in all respects (position and intensity of transitions throughout the entire spectrum). In addition, the optical spectrum obtained for compound **3** is very similar to that of the previously described 8 kDa Au:S(*n*-hexyl) cluster compound[7a] (Figure 4), which is the smallest hydrophobic Au:SR compound of appreciable stability to be isolated. The close agreement of these "matched" pairs of spectra suggest common molecular identities (i.e., core composition and structure), regardless of their respective R groups, preparation methods and yields.

3. Reaction Kinetics. The cluster-formation reaction kinetics could easily be followed by optical densitometry measurements of the electrophoresis gel lanes from the separation of mixtures produced by quenching the reaction at various times. The reaction time dependence, shown in the semilogrithmic form in Figure 5, was obtained by measuring the optical extinction through the gel lanes with a broadband densitometer. The larger clusters have a greater extinction coefficient in much of the visible region, so the yields (based on optical extinction) are biased toward the larger cluster compounds (**4** and **5**), when compared to gravimetric determination (Table 1).

Formation of the Au:SG cluster compounds followed the same general trend as their hydrophobic analogues, where very

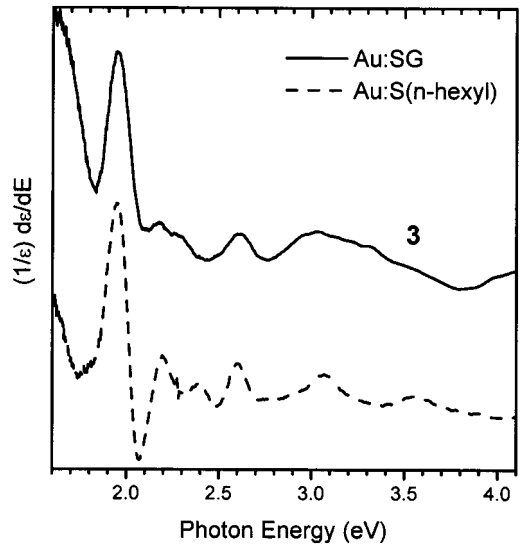

Figure 4. Comparison of optical spectra from ~8 kDa clusters prepared with glutathione (solid line) and *n*-hexanethiol (dashed line). The spectra are shown as the logrithmic differential and offset to facilitate comparison.

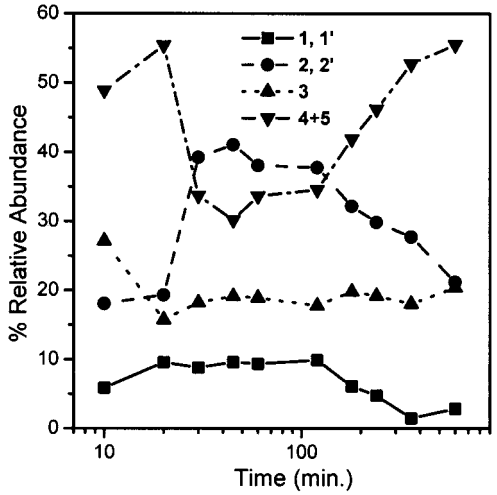

Figure 5. Reaction-time dependence of cluster yields, estimated from optical densities. See Table 1 for gravimetric determination of product abundances for 60 min reaction.

short as well as longer reaction times produced larger cluster compounds.[19,20] The smallest cluster compounds (**1**, **1′**) were never produced in large abundance (no more than 10 wt %). At reaction times of 30 min to 3 h the bands **2**, **2′**, and **3** were produced in largest abundance. At long reaction times (>4 h), increasing abundance of the larger cluster compounds (**4** and **5**) was evident, but was also accompanied by an onset in the production of much larger compounds (colloidal gold), which were nearly immobile on the gel [these were seen as short (2 mm), dark red streaks at the beginning of each lane that could not be removed from the gel for analysis].

4. Mass Spectrometry. Figures 6 and 7 show MALDI mass spectra obtained for the various bands of the mixtures as separated by the low-density and high-density gels. The main features observed in each frame of Figure 6 are (i) a principal broad band at high mass (4−15 kDa equivalent to ~20−80 Au atoms) with some superimposed fine structure for the high-mobility, low-mass compounds; (ii) secondary high-mass bands at multiples of the principal band mass, and (iii) low-mass peaks, below 1.5 kDa, which can be assigned to very small $Au_N(SG)_M$ fragments ($N,M < 5$). Clearly, the mass of the principal band is inversely correlated with the mobility of the components as well as to the onset energy for optical absorption.

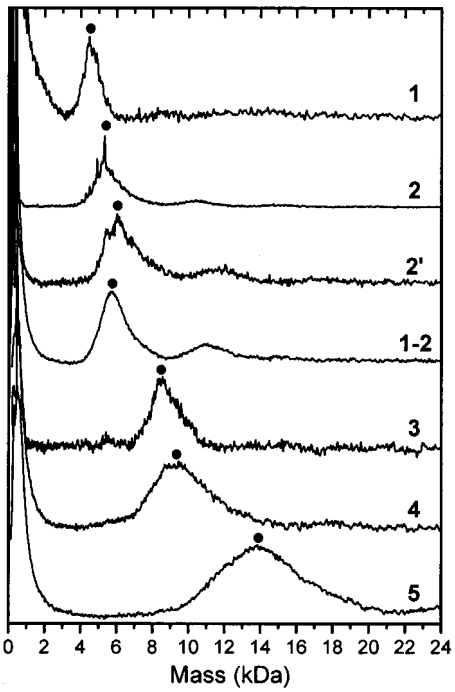

Figure 6. MALDI mass spectra of Au:SG cluster compounds separated by PAGE. Spectra labeled **1**, **2**, **2′**, and **3** were separated under HD conditions, and **1**−**2**, **4,** and **5** under LD conditions. Dots above primary peaks correspond to masses reported in Table 1.

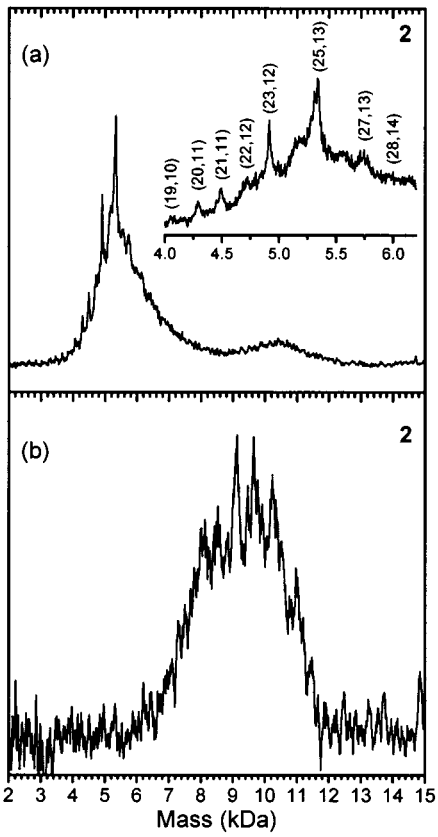

Figure 7. High-fragmentation (a) and low-fragmentation (b) MALDI mass spectra of **2**. High analyte:matrix ratio (1:100) resulted in higher fragmentation, yielding information concerning the inorganic core composition. Low analyte:matrix ratio (1:1000) produced higher mass ions that are consistent with the molecular weight measured by ESI-MS (see Figure 8).

It has been shown previously that, under UV irradiation, the S−C bond in the adsorbed thiol (*RS*−) is efficiently cleaved, and so such laser-desorption mass spectra typically indicate only the composition of the inorganic core (Au_NS_M) and fragments therefrom.[21] Figure 7a shows the identification of the sharp features comprising the principal broad band produced by MALDI of compound **2**, which was separately confirmed by high-resolution mass-spectrometric analysis.[22] Figure 7b is a second MALDI mass spectrum of the same sample, but under conditions of extreme dilution in the matrix host; the principal band of peaks in the spectrum is shifted from 5.4 kDa to higher mass and spans a much wider mass range, from ca. 7 to 11 kDa, and the peak structure can no longer be assigned to a simple combination of Au and S atoms. This result can be interpreted in the following way: Most of the incident UV radiation is absorbed by the matrix, rather than the clusters, thereby mitigating the S−C bond-breaking pathway. The high-mass cutoff of the peak, in the 10−11 kDa region) may approach the intact parent mass of the compound. The broad, complex distribution of peaks in the 7−10 kDa region represents its fragmentation pattern, expected to be dominated by the thermal channel of GSSG loss (612 amu). Of course, the goal is to obtain the mass(es) or molecular weights of the parent compound(s) present in each separated component, but this has not yet been possible by the UV MALDI-MS route.

Figure 8 shows a typical electrospray ionization mass spectrum (ESI-MS) of the same sample. This result has been used to establish a parent mass of **3** as 10 417 amu, as was reported briefly,[16] which is in excellent agreement with the formulation $Au_{28}(SG)_{16}$. (This value is consistent with the MALDI-MS spectrum, Figure 7b, if one allows for the attachment of a few matrix molecules in the MALDI spectrum.) Negligible quantities of other parent-mass species are detected in these mass spectra. The other mass-spectral features, observed as single sharp peaks in Figure 8a, can be assigned to expected low-mass fragments produced in the ionization processes. In particular, the species of highest abundances, $Au(SG)_2^-$ and $(AuSG)_4^{2-}$, have precedents in the structural and ESI-MS literature on nonmetallic aurothiol compounds and mixtures thereof.[23] Consistent with expectations, the ESI mass spectrum of **2** could be changed systematically by addition of a small amount of ammonium hydroxide (∼0.1 mM) to the electrosprayed solution. The signal intensity of negative ions increased for the higher charge states, so that −9, −8, and −7 were highest intensity, and the molecular weight increased slightly, consistent with the presence of NH_3 adducts.

B. Optical Spectroscopy. Figures 9−11 show the complete optical absorption spectra for **1**−**3**, respectively, in dilute aqueous solution, along with their CD spectra. In Figure 12, the optical spectra of **1**−**3** are displayed on a common logarithmic scale, allowing their characteristic features to be compared. The shape and features of the absorption spectra of **1** and **2** are similar, with both showing (i) a distinct absorption onset followed immediately by a shoulder on a broad absorption maximum and (ii) a steep rise into the UV with steplike features superimposed. The discreteness of the optical features of **3** is less pronounced, but still shows the steplike character in the absorption spectrum. The measured optical gaps for compounds **1**, **2**, and **3** are ∼1.7, 1.3, and 1.0 eV, respectively (see arrows, Figures 9−11), where the gaps for **1** and **2** are the largest yet measured for any stable Au:SR cluster compound.

Since circular dichorism requires not only rotation of linearly polarized light but also the presence of a (discrete) electronic transition, the circular dichroism spectra of the Au:SG compounds are exceedingly informative (Figures 9−11, upper curves). All the components separated by electrophoresis showed measurable optical activity (Figure S3), but large chiroptical effects in the near-IR/visible regions were only observed for compounds (**1**−**3** and **1′**, **2′**). The CD spectrum of the reduced glutathione (GSH), shown as an inset in Figure 9, shows no CD response below 5.2 eV.

The magnitude of the CD effect for an electronic transition is directly related to the product of the electric dipole and magnetic dipole transition moments, and thus is also proportional to the optical absorption. Furthermore, it is quite unusual for

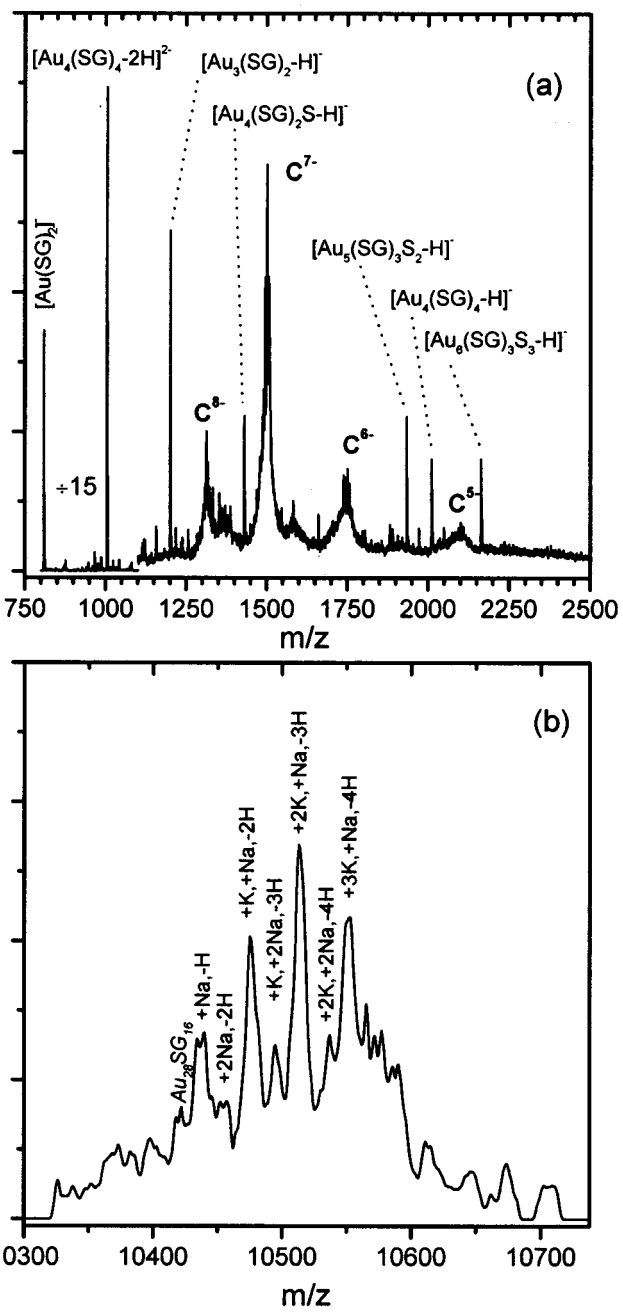

Figure 8. Electrospray ionization mass spectrum of **2**. In the ESI-MS (a), the −5, −6, −7, and −8 charge states were each seen as a group of 5−6 peaks spaced closely together. The "deconvoluted" spectrum (b) shows that a progression of peaks corresponding to various sodium and potassium adducts starting at mass 10 417. The starting peak and subsequent sodium and potassium adduct peaks are most consistent with the compound having a composition of $Au_{28}(SG)_{16}$. The labels in (a) denote various low-molecular-weight fragment ions that are still present even under this gentle ionization method.

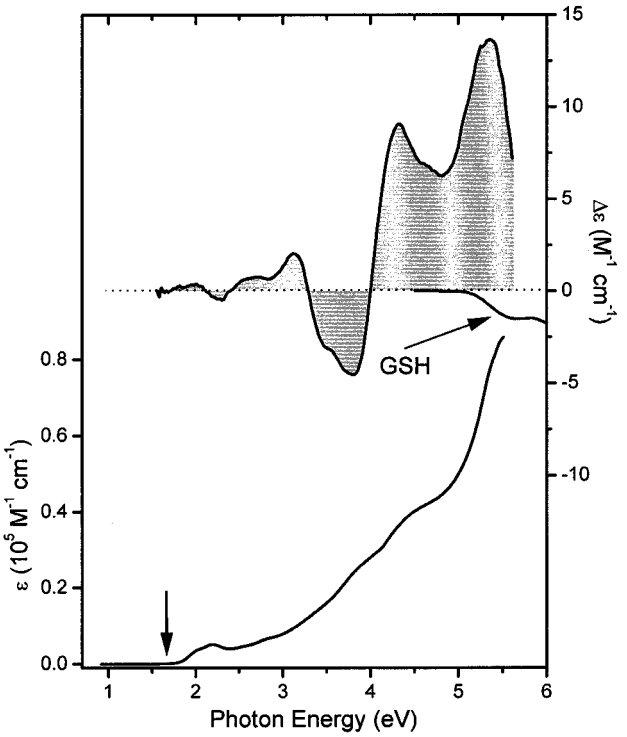

Figure 9. Optical absorption spectrum (lower, left axis) and circular dichroism spectrum (upper, right axis) of **1** in aqueous solution. The solid line in the UV region of the CD corresponds to the CD spectrum of glutathione (i.e., GSH, not bound to Au cluster).

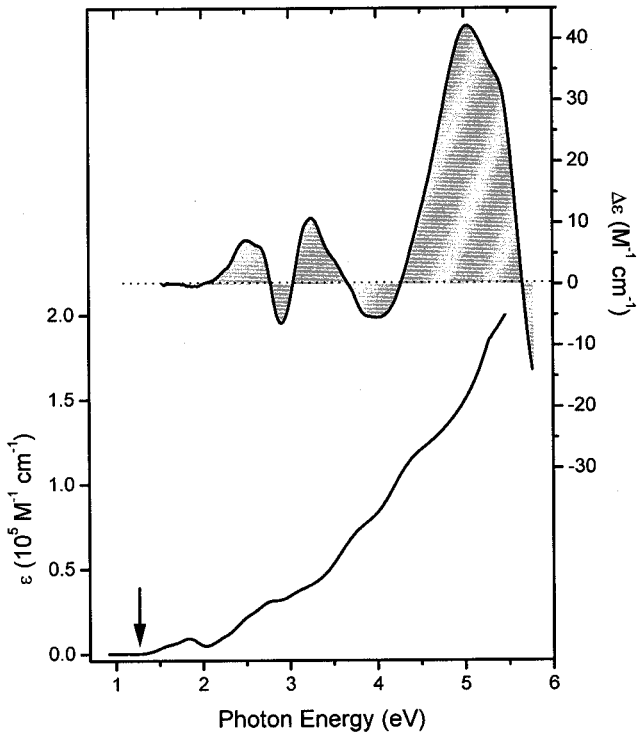

Figure 10. Optical absorption spectra (lower) and circular dichroism spectrum (upper) for compound **2**. Axes are as for Figure 9.

CD spectra of molecules to have features spread over such a large energy range and large range in molar absorptivity. It is therefore justified, both theoretically and practically, to present the *relative* differential absorption spectra (i.e., $\Delta\epsilon/\epsilon$ vs photon energy), which is represented in Figure 13a−c for **1**−**3**, respectively. In these spectra, the various bands are easily identified across the entire spectral range: The relative CD of

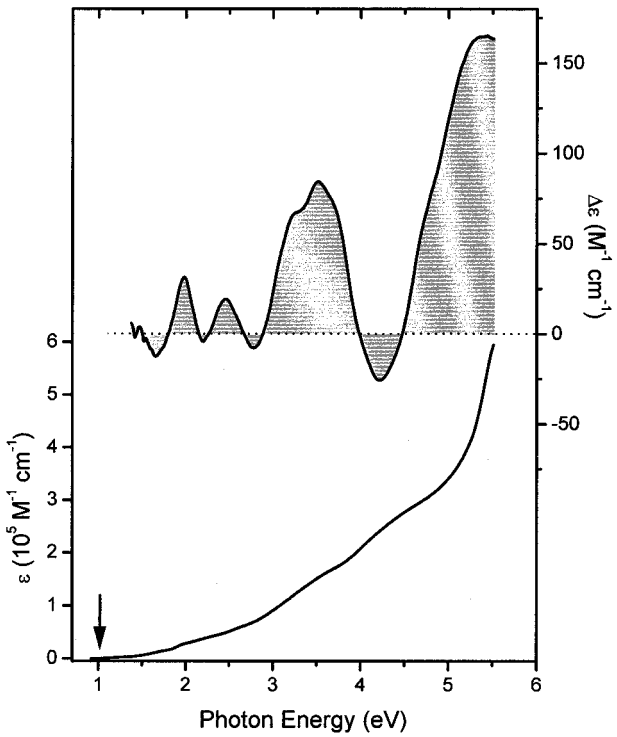

Figure 11. Optical absorption spectra (lower) and circular dichroism spectrum for compound **3**. Axes are as for Figure 9.

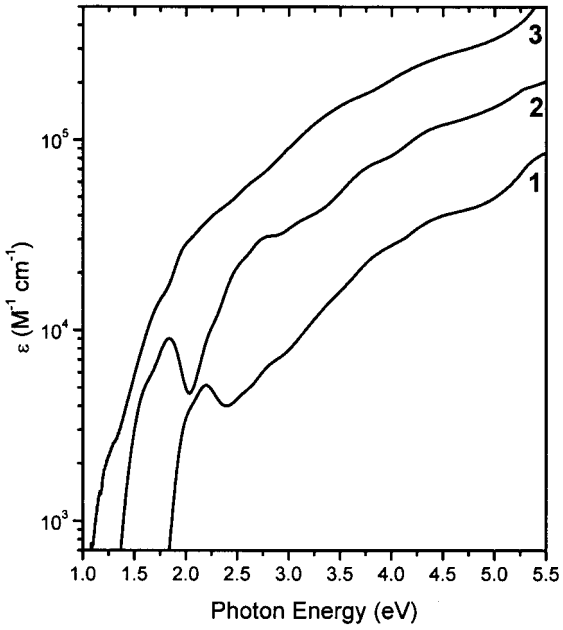

Figure 12. Optical absorption spectra for compounds **1**−**3**, from bottom, plotted on a common logrithmic scale to facilitate comparisons between the spectra.

bands from **1** are in the range of 100−300 ppm; **2** is in the range of 200−400 ppm; **3** is up to over 1100 ppm.

On close inspection, each of the positive and negative Cotton effects present in the CD of the Au:SG compounds correlate directly to most of the features resolved in the absorption spectra of **1** and **2**; however, the discreteness of the absorption spectrum of **3** is substantially less, and direct correlation is not as obvious in this case. To facilitate the discussion and comparisons to archetypal compounds (below), Table 2 presents values for the strongest chiroptical features observed for compounds **1**, **2**, and **3**, including (i) energy of occurrence, (ii) absolute absorbance (ϵ), (iii) differential absorbance ($\Delta\epsilon = \epsilon_R - \epsilon_L$), and (iv) the

TABLE 2: Spectral Features and Constants for the Au:SG Cluster Compounds

	energy (eV)[a]	$\Delta\epsilon$ (M^{-1} cm^{-1})	ϵ (M^{-1} cm^{-1})[b]	$\Delta\epsilon/\epsilon$ (ppm)
	4.34	9.1	36 700	248
1	3.81	−4.6	24 100	−189
	3.50	−3.1	16 000	−195
	3.13	2.0	9500	213
	3.25	10.8	41 000	264
2	2.67	−6.2	27 600	−223
	2.50	7.2	21 700	333
	2.26	2.4	10 700	226
	3.51	84.5	152 000	556
3	3.26	67.5	122 800	550
	2.00	31.3	27 900	1121
	1.66	−12.5	11 300	−1106
	3.81	200	33 000	6000
H1[c]	3.49	70	12 000	6000
H2[d]	2.85	20	10 000	2000
	3.06	210	24 000	8700
C_{76}[e]	2.16	−106	10 000	−10 000

[a] From the negative and positive Cotton effects seen in the circular dichroism. [b] Absorbance at wavelength specified. [c] Hexahelicene.[35] [d] Heterohelicene.[36] [e] Reference 13b.

relative differential absorbance ($\Delta\epsilon/\epsilon$) expressed in parts per million (ppm).

Discussion

By producing cluster compounds that mimic certain chemical and structural properties of large biological molecules, such as proteins,[24] techniques that are used successfully to characterize biomolecules can be employed in the same manner to study the giant Au:SG cluster compounds. The electrophoretic separation of the Au:SG cluster compounds is suggestive of the conceptual picture of the compound's structure and properties, in which a dense inorganic core (Au:S) is surrounded by a polypeptide monolayer of G groups. Thus, the cluster assembly takes on the chemical properties of a polyelectrolyte molecule, similar to a folded globular protein or DNA oligomer molecule. This approach has also been useful in the interpretation of results from a 22 kDa amide-functionalized Au:PR_3 cluster compound, which was separated by liquid chromatographic methods and studied successfully by MALDI-MS.[15]

The mass spectrometric methods typically used to measure the molecular weight of intact protein and DNA ions have thus far produced a total molecular weight value for compound **2**. However, the information gained from the high fragmentation MALDI-MS not only confirms the extent of separation but also provides an estimate of the inorganic core size, thus allowing one to correlate the optical and electronic properties with the inorganic core size of the cluster assembly. Since it is evident, by direct comparisons such as that in Figures **3** and **4**, that the electronic structure of the inorganic core is insensitive to the tail of the adsorbate thiol, this correlation has been of the utmost importance in understanding the evolution of optical properties as related to cluster size. The Au:SG clusters differ from their hydrophobic counterparts: Straight laser-desorption mass spectrometry (UV irradiation of neat films) failed to yield useful information on the composition of the cluster compounds, but rather appeared to result in the complete degradation of the sample. This difference may be explained by the greater cohesion of an ionic solid over a van der Waals molecular solid. Complete degradation could be avoided by diluting the clusters in a suitable UV absorbing matrix and irradiating (MALDI).

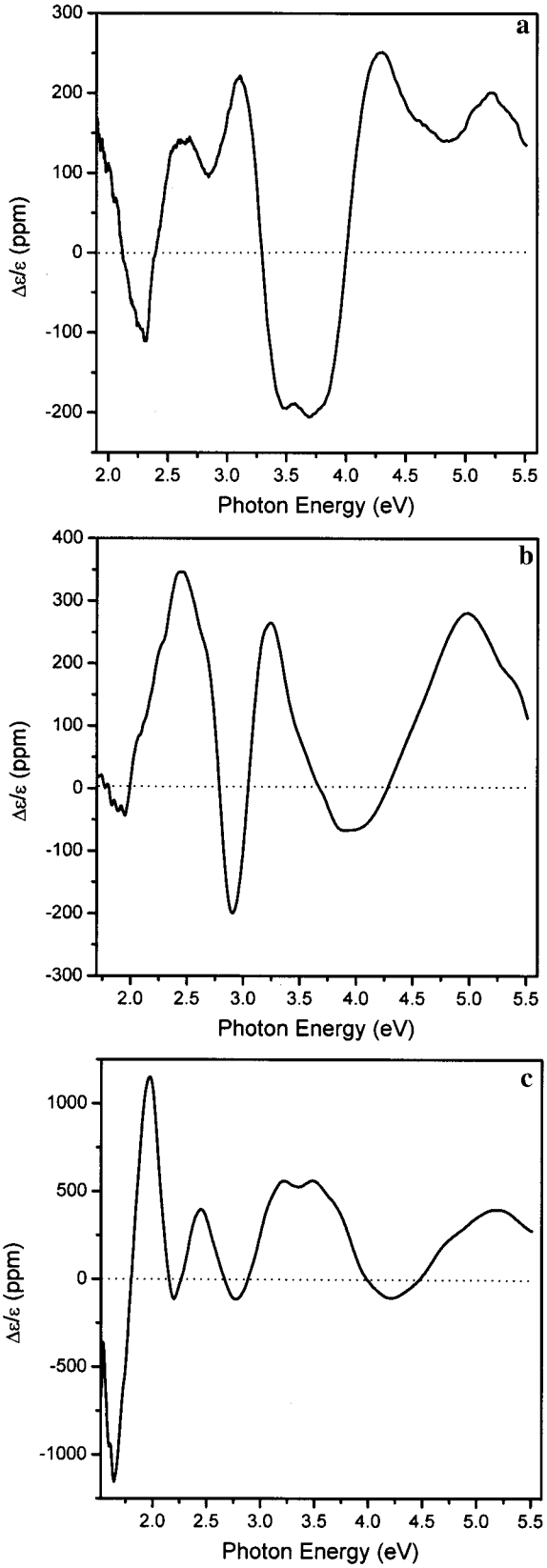

Figure 13. (a) Relative differential absorption spectrum for compound **1**. The spectrum was generated by dividing the CD spectrum (upper curve in Figure 9) by the optical absorption spectrum (lower curve in Figure 9). (b) Relative differential absorption spectrum for compound **2**. The spectrum was generated by dividing the CD spectrum (upper curve in Figure 10) by the optical absorption spectrum (lower curve in Figure 10). (c) Relative differential absorption spectrum for compound **3**. The spectrum was generated by dividing the CD spectrum (upper curve in Figure 11) by the optical absorption spectrum (lower curve in Figure 11).

The ESI-MS analysis of compounds **1** and **3**, although incomplete, is expected to provide intact parent-mass information for these also.

Optical Absorption Spectra and Electronic Structure. The optical spectra of the Au:SG clusters are easily distinguished from those of larger (≥2 nm) Au:SR cluster compounds that have a single, broad "plasmon" band centered at ∼520 nm (2.5 eV), as well as from the spectra of smaller cluster compounds such as those based on the "undecagold" Au_{11}^{3+} core, which have strong blue UV absorption bands, but no red or near-IR absorption.[25] The steplike structure in the optical absorption spectra (see Figure 12) suggests a degree of electronic level quantization that has not been previously shown for the larger Au:SR cluster compounds. While Kubo's statistical formula[26] has been used to qualitatively account for features found in the optical spectra of the 14, 22, and 29 kDa (core mass) Au:SR compounds,[7] this method is inadequate in describing the optical absorption spectra for the smaller cluster compounds. Most important is the emergence of a large optical gap (lowest energy at which absorption occurs). A comparison of optical and electrochemical charging properties has demonstrated a remarkable correlation between this onset energy and the "charging gap" between successive redox transitions, leading to the conclusion that the optical gap may reflect the actual HOMO−LUMO gap emerging in the remnants of the 6sp conduction band.[2] The opening of both optical and electrochemical gaps of the same magnitude suggests that selection rules in the electronic transitions are not playing an integral role in the measurement of the optical gap; i.e., transitions near the HOMO−LUMO transition are not strongly forbidden. Thus, for these smaller cluster compounds, a direct estimate of the HOMO−LUMO gap is accessible and is found to be much larger than the mean energy-level spacing of a metal sphere of this dimension.

The observation of a HOMO−LUMO gap far greater than the statistical estimate requires an explanation as to the origin of the gap. Without total structure determination and ab initio quantum calculations thereupon, the exact origin of the electronic transitions corresponding to the features in the optical spectrum can only be guessed at. However, from a chemical thermodynamics perspective, this type of optical behavior is consistent with the high-yield formation *and* isolation of stable cluster compounds. For example, the magnitude of the band gap or HOMO−LUMO gap in higher fullerenes has been implicated in their inherent stability. The inability to isolate certain small band gap fullerenes (C_{74}, C_{80}) in neutral form by chromatographic methods arises because they are too reactive to survive the separations process.[27] The opening of a substantial HOMO−LUMO gap may be viewed as an expected[28] or even *necessary* condition for the stability and inertness of sufficiently small Au:SR cluster compounds, drastically retarding the rate of atom addition (or removal[29]). Likewise, the matching of the optical absorption spectra (Figures 3 and 4) observed for Au:SG and Au:SC6 compounds sharing the same core mass (as estimated by MALDI-MS and LDI-MS) suggests a preferential formation of certain "special" sizes of Au cores, regardless of the reaction medium and adsorbate tailgroup. The optical gap seen in the absorption spectra also coincides with the onset of chiroptical properties seen for the Au:SG compounds, the interpretation of which is discussed in the following subsection.

CD Spectra, and the Origin of Chiroptical Properties. As a differential spectroscopy, CD provides additional information on each electronic transition of a molecule. Here, the band structure in the CD spectra and the frequent changes in sign make it untenable to regard the optical spectra as the smeared-out remnants of a single "plasmon resonance" (or collective transition). Instead, they call for a detailed assignment of a long series of distinct electronic transitions, involving also comparisons with theoretical calculations at a variety of levels of sophistication. Unfortunately, such theory requires structural hypotheses for the larger clusters, and to our knowledge such a calculation has not even been attempted. For example, the simplest such calculation might involve placing the conduction electrons in a spherical jellium background potential that is perturbed by addition of a weak potential of symmetry appropriate to induce chirality.

In making any such comparisons it is necessary, of course, first to remove from the experimental spectra the simple, additive contributions to the CD spectra from the adsorbate SG groups. These contributions affect only the deep ultraviolet region, which in any case is not the region of primary interest with regard to transitions involving the Au conduction-band electrons. The Au:SG composition ratio is estimated to lie in the 1.5−2.0 range or ca. 12−20 SG units present on each cluster compound (**1**, **2**, **3**), so their contributions, on a per mole-cluster basis, may be significant in the deep-UV region. Conversely, it seems quite certain that, in the 2.5−5 eV region, the strong interband transitions originating in the filled 5d (core) band and terminating in the 6sp valence (conduction) bands dwarf the absorptions derived from the glutathione adsorbates. Specifically, in regard to all the forms of glutathione (GSH, GS^-, and GSSG): These are natural products, possessing chiral centers, namely the α-carbon sites in the glutamyl and cysteinyl residues, and also the S−S bond in GSSG.[30] The reduced form, GSH, is optically transparent below 5 eV[31] and produces a relatively weak (∼1.5 M^{-1} cm^{-1}) CD response (see Figure 9). GSSG has a broad and weak (0.4−0.5 M^{-1} cm^{-1}) CD response spanning the 4.2−5.5 eV range arising from the disulfide π(S−S) → σ^*(S−S) transitions, which are very sensitive to the C−S−S−C dihedral angle. The Cotton effect at shorter wavelengths (202 nm) for GSSG is extremely strong, $\Delta\epsilon \approx -12$ M^{-1} cm^{-1}. Thus, the conceivable *direct contributions* from the GS adsorbate should be (i) negligible at energies below 4 eV, (ii) small, but possibly observable, in the 4.2−5.5 eV region only if GSSG is the adsorbate,[32] and (iii) strong to dominant at higher energy, especially if GSSG pairs are the adsorbate unit.[33]

Generally, in the absence of a total structure determination, one cannot decide among the classes of explanations for the intense optical activity in the near-IR−vis−near-UV regions, i.e., in the transitions of the metal core. These potential explanations can be listed, in order of decreasing intensity as follows: (I) the structure of the metal-cluster core is inherently chiral; (II) the adsorption of the SG groups on the core's surface results in a chiral pattern of adsorbate interactions with an inherently achiral core; (III) chiral elements of the adsorbates induce optical activity in the core electronic structure, even though neither the adsorption pattern nor the core structure is chiral.

We now briefly consider the precedents for each of these, in the above order:

I. Inherently Chiral Cores. Such structures have not been definitively established for larger metal cluster compounds. (Very small cluster compounds, containing typically four or fewer atoms, have been investigated for chiroptical properties, but these seem to belong to a different class of physical systems.) It remains only to point again to the recent precedents for inherently chiral atom-packing structures (Figure 14): Recently theoretical[10] and experimental[11] evidence has shown that bare

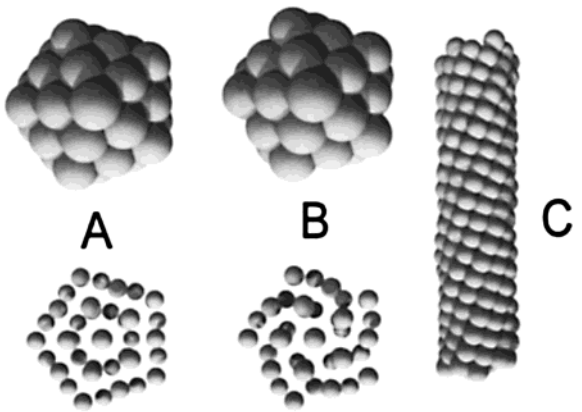

Figure 14. Achiral and chiral structural motifs for nanometer-scale metal structures: Structure A represents an achiral 39-atom structure of D_{5d} symmetry and approximately truncated-decahedral morphology and B represents the chiral 39-atom structure of D_5 symmetry, related to (A) by twisting about the 5-fold symmetry axis as per ref 10. In A and B, the clusters are shown at full van der Waals radii in the top view, and the smaller radii in the bottom view facilitates the comparison between the achiral and chiral structures. Structure C illustrates a compact helical nanowire, after Tosatti et al.[12] The dimensions coincide with those of the Au:SG compound **3**.

Ni_{39} clusters (Figure 14, A and B) prefer a lower (chiral) symmetry (D_5). Likewise, calculations performed on nanometer-scale wires suggest a preferential formation of helical-type structures (Figure 14C). Thus, the optical activity of the Au:SG compounds raises the question: must cluster compounds (of 20−40 atoms) possess highly symmetric structures as previously believed and predicted, or can they take on lower symmetry and even chiral structures?

The relative differential absorption values (Table 2) provide a way to assess the reasonableness of this proposition. In this regard, the chiral fullerenes[13b] and the larger helicenes[34] seem to be the most comparable to the Au:SG cluster compounds, because their optical absorption spectra consist of several overlapping electronic transitions across the near-IR and visible as well as ultraviolet regions (see Table 2 for ϵ, $\Delta\epsilon$, and $\Delta\epsilon/\epsilon$ values). The optical properties of these molecules are derived from the semimetallic bands of graphite, with one pπ electron per atom contributing to delocalized electronic states. The prototypical hexahelicene ($C_{26}H_{16}$) absorbs only in the UV[35] and has $\Delta\epsilon/\epsilon$ values of near 6000 ppm for two band maxima, 355 and 325 nm ($\Delta\epsilon$ = 70 and 200 M^{-1} cm^{-1}, respectively). In **3**, the largest $\Delta\epsilon$ value below 4 eV is 85 M^{-1} cm^{-1}. A more relevant comparison is to a blue-absorbing, much larger heterohelicene,[36] with alternating benzene and thiophene units. Its continuum-like absorption spectrum has a $\Delta\epsilon_{max}$ near 15 in the visible where $\epsilon \approx 10\,000$ M^{-1} cm^{-1}, giving a $\Delta\epsilon/\epsilon$ in the 1000−2000 ppm range, comparable to compound **3**. The prototypical chiral fullerene, D_2−C_{76},[37] has an optical spectrum quite similar to that of compound **2** ($Au_{28}(SG)_{16}$) both in terms of the absorption onset (1.3 eV) and strength of bands. However, the largest $\Delta\epsilon$ values of C_{76} in the visible are $\Delta\epsilon$ = +210 (406 nm) and −106 (578 nm) M^{-1} cm^{-1},[37b] which are twice those found for the Au:SG compounds. From these comparisons, it is evident that the chiroptical effects in compounds **1**−**3** are very large and comparable to that which arises from the delocalized (conduction) electrons of intrinsically chiral structures. However, the larger species (**4** and **5**) show little activity (Figure S3), nor have larger cluster compounds or colloids been reported to exhibit CD even in the presence of chiral adsorbing groups.

II. Chiral Adsorption Pattern. In this mechanism, the cluster core has a structure that is inherently achiral, but the thio headgroups adsorb in a spatial pattern that is chiral. Such a mechanism is plausible and readily envisaged, e.g., a helical tiling on a cylindrically symmetric cluster core. Depending on the nature and strength of the cluster−adsorbate interaction, one can imagine a strong effect on the gold electronic structure. In the precedent provided by the fullerenes, the Cotton effects from a chiral adsorption (adduct) pattern (II) are comparable to those resulting from mechanism (I). However, these involved σ-bond formation that breaks the pπ-conjugation of the fullerenes at specific carbon atom sites. It seems unlikely to us that the adsorption of thio groups on gold surfaces can have such a profound local effect on the electrons, although the actual nature of the metal−adsorbate interaction in Au:SR SAMs remains an unresolved and controversial subject.

III. Chiral Adsorbates Only. In this mechanism, both the adsorption patterns of headgroups and the structure of the core are assumed to be achiral, so that the only remaining stereogenic elements are the chiral centers in the tripeptides discussed above. Their direct, or through-space, influence on the electronic structure of the metal core electrons would be difficult to estimate. However, in the precedents provided by the derivatized fullerenes, induced optical activity of this type produced only weak CD responses (extremely small relative differential absorption) in transitions originating from the fullerene electronic states.[13b] By analogy, we consider (III) to be unlikely to be capable of producing the strong CD responses in the metal-based electronic transitions.

Conclusions

In this report we have shown that gold clusters generated by the reduction of Au(I)SG polymers (GSH = glutathione), can be efficiently separated by electrophoresis to yield a series of distinct compounds in the 20−80 atom range. The emergence of discrete electronic transitions seen in the optical spectrum and corresponding chiroptical effects in the CD was only revealed when the various cluster compounds were separated. The mixture, as obtained simply from the reduction of the precursor Au(I)SG polymer, did not show the strong quantum-size effects in the optical absorption spectra, nor the strong chiroptical effects in the CD. Thus, the elucidation of these optical properties further emphasizes the importance of separations for determining the electronic properties of this class of nanostructured clusters and related materials. While the precise structure of Au:SG cluster compounds and their hydrophobic Au:SR analogues remains a question for total structural determination methods, a further understanding of the properties of this inorganic cluster system has been realized more effectively through rigorous size separations. Studies of mixtures of Au:SR cluster compounds (both hydrophobic and hydrophyllic) have suggested the presence of interesting and potentially valuable properties;[38] however, the enhancement of these properties upon the size separation of mixtures is a more convincing argument for the further exploration of this class of materials. For example, many studies have implicated that the catalytic activity of gold clusters is greatly enhanced at low temperatures for cluster diameters below 2.0 nm (less than 200 atoms).[4] The (supported) cluster size for onset of catalytic activity correlates well to our measurements of the emergence of discrete electronic transitions seen in the size-separated cluster compounds at room temperature.[7]

The optical properties of the separated Au:SG cluster compounds (core sizes ranging from ∼20−40 atoms) and the

previously separated hydrophobic Au:SR compounds (∼40−800 atoms) present a rather complete picture of the evolution of electronic structure as it relates to the number of atoms in the cluster core. In total, nine distinct Au:SR samples (R = *n*-alkyl), with core masses ranging from 8 kDa (∼40 Au atoms) to 165 kDa (∼800 Au atoms), have been separated and their optical properties reported.[39,40] At sizes above ∼200 atoms (>1.8 nm), the Au:SR cluster compounds exhibit optical properties similar to classical colloids, i.e., continuum optical absorption spectra with a broad plasmon centered at ∼520 nm (2.5 eV) that decreases in magnitude (and broadens) upon going to smaller sizes.[39] In the intermediate core-size range (∼70−140 atoms), the optical spectra are semicontinuous with superimposed steplike features that can be enhanced by either measurement at cryogenic temperatures or more easily discerned by taking the mathematical derivative of the optical spectra.[7] Finally, at the smallest Au:SR and Au:SG cluster core sizes isolated (<70 atoms), the (semi-) continuous optical absorption spectra give way to spectra composed of many overlapping discrete electronic transitions that are observable at room temperature. Thus, *when the mixture is separated* into its respective components, this class of compounds exhibits the core-size-dependent optical properties that have been predicted for small bare metallic clusters—the emergence of discrete energy levels upon going to smaller sizes, i.e., quantum-size effects. However, unlike their previous gas phase analogues, these compounds can be prepared and isolated in large quantities.

In particular, the optical response and optical activity of the gold:glutathione cluster compounds place these novel cluster compounds in a class similar to that of the higher fullerenes. More significantly, the novel possibility that lower-symmetry metal cluster structures, possessing a pronounced chiral or helical character, seems not to have been previously considered. In light of experimental evidence[11] supporting the presence of 39-atom Ni clusters having structural characteristics that could give rise to optical activity, this seems to warrant further exploration. The Au:SG family of compounds promise to provide an ideal system for determining the presence of such structures due to the ease of preparation and separation, as well as the robust thermal and chemical stability of these clusters. Until the core and surface structure is known precisely, the exact origin of the optical activity cannot be determined for this system. However, from the preliminary crystal growth seen in the highly purified compound $Au_{28}(SG)_{16}$,[16] the prospects of single-crystal structural determination seem likely.

The broader significance of our results can be appreciated by considering the following three points: (i) To our knowledge, these are by far the largest metal-cluster compounds to show significant optical activity distinct from that of the adsorbate chromophores. (ii) Similarly, the use of a differential spectroscopy on large metal cluster compounds has revealed greatly enhanced electronic structural information over that of absorption alone. (iii) Features in the optical absorption and CD spectra may be useful as spectral fingerprints for identification of intermediates in the biogenic recovery of gold or the use of these compounds as bioconjugate probes.

Note Added in Proof. In their computational investigation of the structure of nickel clusters, Wetzel and de Pristo[10] also reported a remarkably compact 28-atom structure (as the lowest-energy form) that appears to be chiral (assigned to *T* point group). Although we are not aware of any experimental evidence in support of this structure (unlike 39-atom structure[11] shown in Figure 14), it could serve as a plausible model for the core of the $Au_{28}(SG)_{16}$ compound 2.

SCHEME 2

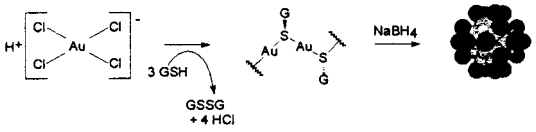

Acknowledgment. Mr. J. Debord, Dr. T. Conti, and Prof. L. Williams provided assistance and advice in this research, which has been supported by the U.S. National Science Foundation and Georgia Tech Research Foundation. The authors also thank S. A. McLuckey, G. Van Berkel, and J. Stephenson at Oak Ridge National Laboratory for the use of the ESI-MS instrumentation and expertise. The authors also thank the Tosatti Research Group for the coordinates of the helical nanowires.

Appendix: Methods

Reaction. The optical activity was revealed by preparing gold clusters through reactions with a chiral thiol, namely the ubiquitous tripeptide glutathione (γ-glu-cys-gly, GSH), and then separating the mixture of cluster compounds by gel electrophoresis as described briefly in ref 16 (see Scheme 2 and discussion above). Typically, 3.0 mmol of glutathione was dissolved in 40 mL of distilled water, and 1.0 mmol of $HAuCl_4$ was dissolved in 80 mL of methanol. Mixing the two solutions generates the previously known Au(I)SG polymer[41] as a cloudy, white suspension. Addition of 10 mmol of $NaBH_4$ in 10 mL of water to this stirring suspension results in an immediate color change to dark brown indicating the generation of large cluster compounds. After additional stirring, the solution was evaporated at 43 °C to near dryness and excess methanol was added to precipitate the clusters and wash reaction byproducts and any remaining starting material. The precipitate was then filtered and redissolved in ∼10 mL of distilled water, precipitated again with methanol, and filtered. These steps were repeated until a fine *black* powder was obtained, and the complete removal of nonadsorbed GSH and GSSG was verified by ^1H and ^{13}C NMR spectroscopy.[16] The reaction, carried out as described, is quantitative, i.e., no bulk gold and no residual Au(I)SG polymer after the reduction step and subsequent purification. The 2:1 methanol:water solution is necessary to prevent uncontrolled growth, i.e., the aqueous reaction resulted in formation of both colloidal and bulk (insoluble) gold. After removal of all starting material and byproducts, the resulting mixture is highly soluble in water (80 mg/mL), insoluble in methanol, and sparingly soluble in dilute methanol.

Isolation (Separations). Isolation of each cluster compound was achieved by polyacrylamide gel electrophoresis (PAGE) (see photo in Figure 1). The running conditions and preparation of the polyacrylamide gel were altered from typical protein conditions to retain the small Au:SG compounds, which are highly anionic and mobile at running pH (8.8). The usual denaturing reagent, sodium dodecanesulfonate (SDS), was unnecessary either in the preparation of the gel or in the eluting buffer solution. One of two acrylamide/bis(acrylamide) monomer concentrations were used to form the gel, depending on the type of separations desired. The gel conditions were either 20% (low density, LD) or 24% (high density, HD) total acrylamide monomer content by weight, with 7% cross-linking bis(acrylamide), which was formed and run under basic conditions (pH 8.8). At such high polymer concentrations, the gel preparation was also altered to prevent excessive heating, which

causes cracking or separation of the gel from the glass plates. (See Supporting Information, Table S1, for conditions and comparison to standard gel preparations.) The eluting buffer consisted of 125 mM glycine: 20 mM tris(hydroxymethyl-amine). The cluster mixture produced by precipitation of the reaction product was then dissolved in a 95:5 water:glycerol solution at a concentration of 4 mg/mL and loaded onto the gel to a height of 3−5 mm. Two different gel widths (thicknesses) were used without any significant difference in the separation effectiveness. A 1.5 mm gel was typically used to analyze synthesis modifications; 30 lanes could be eluted simultaneously. For preparative separations, a 3 mm gel without lanes was used so that ∼1 mL of the 4 mg/mL solution could be loaded onto each of the two gels and run simultaneously (8 mg total separation). The samples were eluted at 150 V, current limited, for 6 h to achieve adequate separation. It was verified by repeated runs that the gel electrophoresis procedures did not modify (or generate) the Au:SG compounds and that each electrophoretically separated component of the mixture had a distinct mobility.

Yield. After elution, the resulting bands were cut out of the gel and placed in distilled water overnight in order to extract each cluster compound from the gel. Then the solution of each separated compound was then concentrated to ∼1 mL and the pH adjusted by adding 1 mL of 2% acetic acid to the solution so that the clusters could be selectively precipitated from the highly concentrated buffer solution by addition of excess methanol. After the separation and subsequent cleanup, typically 60−70% of the total mixture was recovered from the gel in the various fractions. Under fairly tolerant conditions (0.5−3 h reaction time), the cluster compound corresponding to the third most mobile band was produced at 25% yield.

Mass Spectrometry. The matrix-assisted laser desorption ionization mass spectrometry (MALDI-MS) was performed using a reflectron time-of-flight mass spectrometer designed and custom built for LDI and MALDI studies of cluster compounds. A solution containing 3 mg/mL of the separated Au:SG clusters in water was mixed (1:1, v:v) with a 0.1 M solution of (2,5) dihydroxybenzoic acid (DHB) in 1:1 water:methanol (∼1:1000, (Au:SG):DHB). Then 4 μL of this solution was vacuum-dried on the tip of a desorption rod. The sample was immediately inserted into the instrument and irradiated by the third harmonic (355 nm) of a Continuum Nd:YAG pulsed laser. The spectra shown are the average of 30−50 individual waveforms.

Electrospray mass spectra (ESI-MS) were obtained on (70: 30, water:methanol) solutions containing 0.24 mg/mL of the powder produced from the precipitation of the most abundant species found in the separation by electrophoresis. The solution was sprayed at a flow rate of 10 μL/min into a Sciex API-165 LC/MS quadrupole mass spectrometer. The spray was generated under normal operating conditions (4.2−5 kV needle, 100 V orifice voltage). The charged droplets were initially desolvated by a room temperature, countercurrent drying gas (N_2). At the last stage of desolvation, slightly higher voltages (interface CID conditions) were required to completely desolvate the ions before they were injected into the quadrupole mass filter, resulting in a minor amount of fragmentation to low-mass product ions, but still producing in high abundance the intact assembly as multiply charged negative ions.

Spectroscopy. Except for compound **2**, where a precise measure of molecular weight was obtained, the core masses obtained by laser desorption mass spectrometry were used to estimate the molecular weights of each compound for the calculation of molar quantities, e.g., extinction coefficients. The optical absorption spectrum of each species was determined using a Perkin-Elmer Lambda-19 UV−vis−near-IR spectrophotometer at concentrations ranging from ∼0.5 to 20 mg/mL, to verify linear scaling of spectral absorbance features. The circular dichroism of the Au:SG cluster compounds was measured using a Jasco J-20 spectrophotometer on aqueous solutions with concentrations in the same range as the absorption measurements. Substantial dilution was required in the far-UV region (λ < 250 nm) due to the highly absorbing Au core of the cluster compounds. All of the absorption values and Cotton effects measured in the Au:SG compounds scale linearly with concentrations ranging from ∼0.5 to 20 mg/mL. The optical absorption and CD spectra of various Au:SR's with achiral R-groups were taken in hexane solutions under the same conditions.

Supporting Information Available: Preparation of the low- and high-density polyacrylamide gel for electrophoresis separations. Preparation and separation of the 5.6 kDa Au:S(*n*-hexyl) cluster compound. Circular dichroism of all fractions obtained from the electrophoresis separations is plotted versus photon wavelength. This material is available free of charge via the Internet at http://pubs.acs.org.

References and Notes

(1) (a) deHeer, W. A. *Rev. Mod. Phys.* **1993**, *65*, 611−676. (b) Martin, T. P.; Bergman, T.; Gohlich, H.; Lange, T. *J. Phys. Chem.* **1991**, *95*, 6421−6429. (b) Kreibig, U.; Vollmer, M. *Optical properties of metal clusters*; Springer: Berlin, 1995.

(2) (a) Chen, S.; Ingram, R. S.; Hostetler, M. J.; Pietron, J. J.; Murray, R. W.; Schaaff, T. G.; Khoury, J. T.; Alvarez, M. M.; Whetten, R. L. *Science* **1998**, *280*, 2098−2101. (b) Ingram, R. S.; Hostetler, M. J.; Murray, R. W.; Schaaff, T. G.; Khoury, J. T.; Whetten, R. L.; Bigioni, T. P.; Guthrie, D. K.; First, P. N. *J. Am. Chem. Soc.* **1997**, *119*, 9279−9280. (c) Fan, F.-R. F.; Bard, A. J. *Science* **1997**, *277*, 1791−1793. (d) Roth, J. D.; Lewis, G. J.; Stafford, L. K.; Jiang, X.; Dahl, L. R.; Weaver, M. J. *J. Am. Chem. Soc.* **1992**, *114*, 4, 6159−6164.

(3) Clark, H. C.; Jain, V. K. *Coord. Chem. Rev.* **1984**, *55*, 151−204.

(4) a) Torres-Sanchez, R. M.; Ueda, A.; Tanaka, K.; Haruta, M. *J. Catal.* **1997**, *168*, 125−127. (b) Valden, M.; Lai, X.; Goodman, D. W. *Science* **1998**, *281*, 1647−1650.

(5) Collier, C. P.; Saykally, R. J.; Shiang, J. J.; Henricks, S. E.; Heath, J. R. *Science* **1998**, *277*, 1978−1981.

(6) Elghanian, R.; Storoff, J. J.; Mucic, R. C.; Letsinger, R. L.; Mirkin, C. A. *Science* **1997**, *277*, 1077−1081.

(7) (a) Schaaff, T. G.; Shafigullin, M. N.; Khoury, J. T.; Vezmar, I.; Whetten, R. L.; Cullen, W. G.; First, P. N.; Gutierrez, C.; Ascensio, J.; Jose-Yacaman, M. J. *J. Phys. Chem. B* **1997**, *101*, 7885−7891. (b) Khoury, J. T.; Alvarez, M. M.; Schaaff, T. G.; Shafigullin, M. N.; Whetten, R. L., manuscript in preparation.

(8) Cleveland, C. L.; Landman, U.; Shafigullin, M. N.; Stephens, P. W.; Whetten, R. L. *Z. Phys. D* **1997**, *40*, 503−508.

(9) a) Marks, L. D. *Philos. Mag. A* **1984**, *49*, 81−93. (b) Cleveland, C. L.; Landman, U.; Schaaff, T. G.; Shafigullin, M. N.; Stephens, P. W.; Whetten, R. L. *Phys. Rev. Lett.* **1997**, *79*, 1873−1876. (c) Doye, J. P. K.; Wales, D. J. *Chem. Phys. Lett.* **1995**, *247*, 339−347. (d)Doye, J. P. K.; Wales, D. J. *J. Chem. Soc., Faraday Trans.* **1997**, *93*, 4233−4243.

(10) Wetzel, T. L.; De Pristo, A. E. *J. Chem. Phys.* **1996**, *105*, 572−580.

(11) Parks, E. K.; Kerns, K. P.; Riley, S. J. *J. Chem. Phys.* **1998**, *109*, 10207−10216.

(12) Gulseren, O.; Ercolessi, F.; Tosatti, E. *Phys. Rev. Lett.* **1998**, *80*, 3775−3778.

(13) (a) Ettl, R.; Chao, I.; Diederich, F.; Whetten, R. L. *Nature* **1991**, *353*, 149−153. (b) Thilgen, C.; Herrmann, A.; Dieterich, F. *Angew. Chem., Int. Ed. Engl.* **1997**, *36*, 2268−2280.

(14) Iijima, S. *Nature* **1991**, *354*, 56−58.

(15) Guttierrez, E.; Powell, R. D.; Furuya, F. R.; Hainfeld, J. F.; Schaaff, T. G.; Shafigullin, M. N.; Stephens, P. W.; Whetten, R. L. *Eur. Phys. J. D.* **1999**, *9*, 647−651.

(16) Schaaff, T. G.; Knight, G.; Shafigullin, M. N.; Borkman, R. F.; Whetten, R. L. *J. Phys. Chem. B* **1998**, *102*, 10643−10646.

(17) Templeton, A. C.; Chen, S.-W.; Gross, S. M.; Murray, R. W. *Langmuir* **1999**, *15*, 66−76. Templeton, A. C.; Cliffel, D. E.; Murray, R. W. *J. Am. Chem. Soc.* **1999**, *121*, 7081−7089.

(18) (a) Whetten, R. L.; Khoury, J. T.; Alvarez, M. M.; Murthy, S.; Vezmar, I.; Wang, Z. L.; Stephens, P. W.; Cleveland, C. L.; Luedtke, W. D.; Landman, U. *Adv. Mater.* **1996**, *8*, 428−433. (b) Alvarez, M. M.; Khoury, J. T.; Schaaff, T. G.; Shafigullin, M. N.; Vezmar, I.; Whetten, R. L. *Chem. Phys. Lett.* **1997**, *266*, 91−98. (c) Harfenist, S. A.; Wang, Z. L.; Whetten, R. L.; Vezmar, I.; Alvarez, M. M. *Adv. Mater.* **1997**, *9*, 817−822.

(19) (a) Leff, D. V.; Ohara, P. C.; Heath, J. R.; Gelbart, W. M. *J. Phys. Chem.* **1995**, *99*, 7036−7041. (b) Hostetler, M. J.; Wingate, J. E.; Zhong, C.-J.; Harris, J. E.; Vachet, R. W.; Clark, M. R.; Londono, J. D.; Green, S. J.; Stokes, J. J.; Wignall, G. D.; Glish, G. L.; Porter, M. D.; Evens, N. D.; Murray, R. W. *Langmuir* **1998**, *14*, 17−30.

(20) Schaaff, T. G. Dissertation, Georgia Institute of Technology, 1998.

(21) (a) Arnold, R. J.; Reilly, J. P. *J. Am. Chem. Soc.* **1998**, *120*, 1528−1532. (b) Vezmar, I.; Alvarez, M. M.; Khoury, J. T.; Salisbury, B. E.; Shafigullin, M. N.; Whetten, R. L. *Z. Phys. D.* **1997**, *40*, 147−151.

(22) Salisbury, B. E. Dissertation, Georgia Institute of Technology, 1999.

(23) Howard-Lock, H. E.; LeBlanc, D. J.; Lock, C. J. L.; Smith, R. W.; Wang, Z. *Chem. Commun.* **1996**, 1391−1392.

(24) (a) Mann, S. *Nature* **1993**, *365*, 499−505. (b) Mann, S. *Biomimetic Materials Chemistry*; VCH: New York, 1995.

(25) Mingos, D. M. P. *J. Chem. Soc., Dalton Trans.* **1997**, 561−566.

(26) Kubo, R.; Kawabata, A.; Kobayashi, S. *Annu. Rev. Mater. Sci.* **1984**, *14*, 49−64.

(27) Diener, M. D.; Alford, J. M. *Nature* **1998**, *393*, 668−670.

(28) Mingos, D. M. P. *Chem. Soc. Rev.* **1986**, *15*, 31−61.

(29) Schaaff, T. G.; Whetten, R. L. *J. Phys. Chem B* **1999**, *102*, xxx.

(30) Ottnad, M.; Ottnad, C.; Hartter, P.; Jung, G. *Chiroptical properties of glutathione and related disulfides*; Flohe, L., Benohr, C., Sies, H., Waller, H. D., Wendel, A., Eds., Tubingen, 1974.

(31) Thompson, S. D.; Carroll, D. G.; Watson, F.; O'Donnell, M.; McGlynn, S. P. *J. Chem. Phys.* **1966**, *45*, 1367−1379.

(32) The sharp absorption increase seen in the optical spectrum of **1** at ∼4.8 eV coincides with a sharp Cotton effect in the CD spectrum, which may correspond to glutathione disulfide adsorbate molecules.

(33) (a) Fenter, P.; Eberhardt, A.; Eisenberger, P. *Science* **1994**, *266*, 1216−1218. (b) Fenter, P.; Schreiber, F.; Berman, L.; Scoles, G.; Eisenberger, P.; Bedzyk, M. J. *Surf. Sci.* **1998**, *412/413*, 213−235.

(34) Meurer, K. P.; Vogtle, F. Helical molecules in organic chemistry. In *Topics in Current Chemistry*; Boschke, F. L., Ed.; Springer-Verlag: Berlin, 1986; Vol. 127.

(35) Newman, M. S.; Darlak, R. S.; Tsai, L. L. *J. Am. Chem. Soc.* **1967**, *89*, 6191−6196.

(36) Yamada, K., et al. *Bull. Chem. Soc. Jpn.* **1982**, *55*, 500−503.

(37) Kessinger, R.; Crassous, J.; Herrmann, A.; Ruttimann, M.; Echegoyen, L.; Diederich; F. *Angew. Chem., Int. Ed. Engl.* **1998**, *37*, 1919−1922.

(38) (a) Green, S. J.; Stokes, J. J.; Hostetler, M. J.; Pietron, J.; Murray, R. W. *J. Phys. Chem. B* **1997**, *101*, 2663−2668. (b) Terrill, R. H.; Postlethwaite, T. A.; Chen, C.-h.; Poon, C.-D.; Terzis, A.; Chen, A.; Hutchison, J. E.; Clark, M. R.; Wignall, G.; Londono, J. D.; Superfine, R.; Falvo, M.; Jr., C. S. J.; Samulski, E. T.; Murray, R. W. *J. Am. Chem. Soc.* **1995**, *117*, 12537−12548. (c) Hostetler, M. J.; Murray, R. W. *Curr. Opin. Colloid Interface Sci.* **1997**, *2*, 42−50. (d) Schon, G.; Simon, U. *Colloid. Polym. Sci.* **1995**, *273*, 202−218. (e)Schon, G.; Simon, U. *Colloid. Polym. Sci.* **1995**, *273*, 101−117.

(39) Alvarez, M. M.; Khoury, J. T.; Schaaff, T. G.; Shafigullin, M. N.; Vezmar, I.; Whetten, R. L. *J. Phys. Chem.* **1997**, *101*, 3706−3712.

(40) The optical properties of Au: SR clusters with core masses (∼number Au atoms) of 165 kDa (800), 93 kDa (450), 69 kDa (350), 45 kDa (230), and 29 kDa (145) are discussed in ref 39. Their smaller homologues, 38 kDa (190), 29 kDa (145), 22 kDa (110), 14 kDa (70), and 8 kDa (40), are discussed in ref 7a. See also: Whetten et al. *Electronic Properties of Novel Materials—Progress in Molecular Nanostructures*; XII International Winterschool: Kirchberg, Tyrol, Austria, March 1998; pp 403−406.

(41) Shaw, F. C. I.; Schaeffer, N. A.; Elder, R. C.; Eidsness, M. K.; Trootser, J. M.; Calis, G. H. M. *J. Am. Chem. Soc.* **1984**, *106*, 3511.